

# Tissue-Specific and Developmental Modifications of Grape Cell Walls Influence the Adsorption of Proanthocyanidins

Keren A. Bindon,<sup>\*,†</sup> Antony Bacic,<sup>§</sup> and James A. Kennedy<sup>†,⊥</sup>

<sup>†</sup>The Australian Wine Research Institute, P.O. Box 197, Glen Osmond, South Australia 5064, Australia

<sup>§</sup>ARC Centre of Excellence in Plant Cell Walls, School of Botany, University of Melbourne, Victoria 3010, Australia

<sup>⊥</sup>Department of Viticulture and Enology, California State University—Fresno, MS VR89, 2360 East Barstow Avenue, Fresno, California 93740-8003, United States

**S** Supporting Information

**ABSTRACT:** Cell wall material from *Vitis vinifera* L. cv. Cabernet Sauvignon grape skin and flesh was isolated at different stages of grape maturity to determine whether developmental changes in cell wall composition in different tissue types influence the binding of proanthocyanidins (PAs). Trends in cell wall adsorption of, and selectivity for, PAs were determined using two skin PAs that differed in their average molecular masses. Flesh cell walls consistently bound a higher amount of PA than those from skin. Key structural differences that reduced PA adsorption in skin cell walls by comparison with flesh cell walls were endogenously higher concentrations of insoluble PA, Klason lignin, and lower cell wall-bound protein. These differences may confer reduced flexibility and porosity of skin cell walls relative to flesh cell walls. Analysis of skin and flesh cell wall properties revealed that the onset of ripening was associated with a loss of type I arabinogalactan and galacturonic acid, which indicated a degradation of pectin within the cell wall. Flesh cell walls consistently bound PAs of larger molecular mass, and changes in PA adsorption properties after the onset of ripening were minor. For skin cell walls, adsorption of PA was lowest immediately following solubilization of galacturonic acid, and high molecular mass PAs were poorly bound. As ripening progressed, PAs of higher molecular mass were selectively adsorbed by skin cell walls, which indicates that ongoing cell wall remodeling during ripening may confer an increased porosity within the skin cell wall matrix, resulting in a greater adsorption of PA within a permeable structure.

**KEYWORDS:** proanthocyanidin, tannin, lignin, grape, ripening, cell wall, polysaccharide, arabinogalactan, pectin, porosity

## INTRODUCTION

During development, the tissues of the grape berry accumulate significant quantities of proanthocyanidins (PAs). The composition of these PAs depends upon their location within the grape berry. When compared with seed or mesocarp (flesh) PAs, skin PAs are comparatively rich in epigallocatechin (prodelphinidin) as an extension subunit and have a higher average mean degree of polymerization (mDP), that is, molecular mass.<sup>1–3</sup> Skin PAs also display a comparatively large DP, ranging from 3 to >70 subunits.<sup>1,3</sup>

During processing for either vinification, juice production, or bioproduct extraction, the extent to which skin PAs are extracted can be limited by their high adsorption affinity for cell wall material, either in situ within the skin cells or by contact with suspended flesh material.<sup>3</sup> A similar phenomenon has also been observed to occur during apple processing for juice and cider production.<sup>4</sup> Studies using apple mesocarp have revealed that the adsorption affinity of apple PAs for cell walls is not strictly characterized by Langmuir's isotherm; that is, the extent of PA binding is not proportional to the available cell wall binding sites. Instead, the data suggest a dual binding mechanism, in which PAs bind to the cell walls and then interact by secondary hydrogen bonding with further PAs to increase their association with cell wall material.<sup>5,6</sup> This effect has been observed to be enhanced for highly polymerized PAs. These observations make the analysis of cell wall material

adsorption affinity and selectivity for heterogeneous PAs difficult to predict using multivariate modeling.<sup>4</sup>

The use of the gel permeation chromatography (GPC) for the analysis of grape PAs has enabled the rapid characterization of the polydispersity of PA isolates,<sup>7</sup> allowing for the detailed study of selectivity of cell wall materials for heterogeneous PAs within a single sample.<sup>8</sup> However, on the basis of findings from studies on apple PAs and cell walls,<sup>5,6</sup> the GPC technique necessitates the observation of complexes below PA saturation of available cell wall material binding sites and thus approximates the adsorption constant of the material, but does not enable an absolute value to be determined. With this in mind, research using model experiments has shown that grape cell walls have a variable adsorption for skin PAs, as well as differences in selectivity based on their molecular mass.<sup>3,8,9</sup> Flesh cell wall material invariably has a high PA adsorption, in particular for those of higher molecular mass.<sup>8</sup> By mass, skin cell walls generally bind PA less effectively than those from flesh, and under certain conditions those of high molecular mass are poorly adsorbed, contrasting with earlier studies on PA–cell wall interactions in grapes and apples.<sup>3–5,9</sup>

**Received:** April 11, 2012

**Revised:** July 31, 2012

**Accepted:** August 6, 2012

**Published:** August 6, 2012

The modification of cell wall polysaccharide composition and organization has been shown to influence the interaction with PAs. A study of the modification of apple mesocarp cell walls by application of a pectin lyase found that the affinity constant for a heterogeneous, lower (21 units) mDP PA fraction was unchanged, but that affinity for a higher (73 units) mDP fraction was enhanced 3-fold.<sup>5</sup> In a further study, harsh drying of apple cell walls at 100 °C was found to reduce their surface area due to a decrease in porosity, decreasing the affinity constant of the material for PAs per unit mass.<sup>10</sup> Additional studies using model polysaccharides have revealed that the affinity of PAs was greatest for pectin, followed by xyloglucan, and lowest for cellulose.<sup>11</sup> The higher affinity constants observed for pectins were proposed to be due to the formation of a three-dimensional gel-like network, which facilitated the encapsulation of PAs within the polysaccharide structure.<sup>11</sup>

The process of ripening, characterized in many fruits by softening of the fleshy tissues, is primarily due to modifications that occur within the cell wall. In grapes, the changes in cell wall structure involve the solubilization of galacturonan, with a concomitant reduction in the abundance of the arabinogalactan side chains of pectins.<sup>12</sup> It is thought that the loss of these components opens the interior of the cell wall to various degrading enzymes, causing further depolymerization, and an increased porosity. Some variability in the timing and extent of this process has been shown to be cultivar-dependent, and in some cases there is no observable decline in galacturonans after veraison.<sup>13,14</sup> In some grape varieties, ripening has been observed to be accompanied by the deposition of hydroxyproline-rich glycoproteins within the cell wall matrix,<sup>12,13</sup> which potentially have a high capacity for PA adsorption. These dynamic changes may confer distinct differences to the binding properties of cell walls for PAs as grape ripening progresses.

In many cases, the total available PA content in grapes is not related to PA extraction of grape juice and wine. Changes in cell walls that confer differences in adsorption properties for PA might account for some of the observed inconsistency.<sup>3,15,16</sup> To date, only one published study has compared the adsorption of wine PAs by crude fiber extracts from ripening Cabernet Sauvignon flesh and skin tissues.<sup>16</sup> It was found that PA adsorption by fibers increased during the ripening period, but began to decline by commercial harvest. To attempt to characterize these observations in ref 16, the current study aimed to track changes in PA–cell wall isolated from ripening skin and flesh tissues of *Vitis vinifera* L. cv. Cabernet Sauvignon. Due to previous findings that the modification of skin PAs during ripening can affect their binding properties with grape cell walls,<sup>9</sup> two characterized PA isolates from unripe and ripe grape skins were used for the adsorption assays. When distinct differences in PA adsorption were observed between cell wall samples, samples were subjected to a detailed compositional analysis. Data were analyzed using principal component regression analysis.

## MATERIALS AND METHODS

**Instrumentation.** For PA and monosaccharide analysis an Agilent model 1100 HPLC (Agilent Technologies Australia Pty Ltd., Melbourne, Australia) was used. For the analysis of monosaccharides as their alditol acetates a Hewlett-Packard gas chromatograph (6890 series) coupled with a Hewlett-Packard 5973 mass selective detector (Hewlett-Packard Australia, North Ryde, NSW, Australia) (GC-MS) was used. Both methods used Agilent Chemstation software for data analysis (Agilent Technologies Australia Pty Ltd.).

**Grape Sampling and Preparation for Analysis.** *V. vinifera* L. cv. Cabernet Sauvignon samples were obtained from an irrigated (0.5 ML/ha) commercial vineyard in the Langhorne Creek growing region of South Australia, Australia, which has a latitude of 35° 16' 11.56" S and a longitude of 139° 00' 14.47" E, with an elevation approximately 28 m above sea level. The grapevines were 12 years old, planted 2.5 m (row) × 1.8 m (vine), on their own roots, spur pruned, with a single-wire trellis and sprawling canopies. Further details of this study have been previously published.<sup>9</sup> Grape samples were obtained from preveraison (green) to a total soluble solids level of  $\approx 26$  °Brix for the 2009 and 2010 growing seasons. The timing of veraison was January 20 in 2009 and January 26 in 2010. In the second season of the study a wider range of sampling dates was incorporated to confirm previous observations and also to capture information regarding the development stages at, or shortly after, veraison. To obtain a representative vineyard sample, 100- and 200-berry samples were collected from grapevines within three separate rows distributed within the vineyard block. The 100-berry samples were processed fresh and manually separated into skin, flesh, and seed components while kept on ice. Skin and flesh materials were weighed, frozen in liquid nitrogen, and stored at –80 °C until processed. The 200-berry samples were pressed by hand in a small plastic bag to express the juice and then centrifuged at 1730g for 5 min to clarify the juice. The total juice volume was recorded, and the juice total soluble solids (°Brix) were determined using a digital refractometer. This was not done for preveraison samples due to the low juice yield.

**Preparation of Grape Cell Wall Material.** Cell wall material was isolated from frozen skin and flesh samples using an adaptation of previously published methods.<sup>8,17</sup> Frozen flesh was pre-extracted in 30 mL of 40 mM HEPES (pH 7) at 4 °C for 30 min to remove water-soluble material, whereas skin material was not pre-extracted. The flesh samples were then centrifuged twice at 8000g for 20 min at 4 °C, and the insoluble residue was retained. The pre-extraction step was different for flesh and skin due to the expected higher concentration of soluble pectic polysaccharides in flesh.<sup>17</sup> For skin material, the presence of higher relative amounts of PAs<sup>3</sup> would limit the extractability of soluble polysaccharides in the buffer; hence, skin material was extracted with water at a later stage in the isolation process when endogenous enzymes would have been inactivated by the acetone–water extraction step. The HEPES-extracted flesh material and untreated frozen skins were extracted in 70% v/v acetone for 18 h to exhaustively remove PAs. Acetone-extracted residues were washed in additional 70% v/v acetone, followed by Milli-Q water (Millipore Corp., Billerica, MA, USA). Flesh material was observed to be highly fragmented and did not require processing before being further extracted. Skin material required further homogenization and was first lyophilized and then ground under liquid nitrogen with a mortar and pestle. Thereafter, cell wall material was prepared from acetone-extracted skin and flesh residues according to the buffered phenol procedure.<sup>8,17</sup> Recovered, dry cell wall materials were pooled per maturity stage, further ground to a fine powder with a mortar and pestle, passed through a 0.5 mm sieve, and stored at –20 °C.

**Extraction and Preparation of Skin Proanthocyanidins.** Detailed extraction and chemical preparation of PA extracts used in this experiment has been previously published.<sup>9</sup> A preveraison (January 9, 2009) skin PA and a ripe (March 19, 2009) skin PA were selected from that study for use in adsorption experiments with cell wall isolates at different ripeness stages. Grape skin 70% v/v acetone extracts were concentrated under reduced pressure at 35 °C and then extracted with *n*-hexane to remove residual lipophilic material. The aqueous fraction was recovered using a separatory funnel, made up to a final concentration of 60% v/v methanol containing 0.05% v/v trifluoroacetic acid (TFA). This PA-containing solution was then applied ( $\sim 18$  mL/min) to a 300 × 21 mm glass column (Michel-Miller, Vineland, NJ, USA) containing Sephadex LH20 chromatography resin (Amersham, Uppsala, Sweden) to a bed volume of 93 mL and low molecular weight phenolics were eluted with 300 mL of 60% (v/v) HPLC grade methanol containing 0.05% v/v TFA. PA was then eluted with 250 mL of 70% v/v acetone containing 0.05% v/v TFA. The column was re-equilibrated with 60% v/v

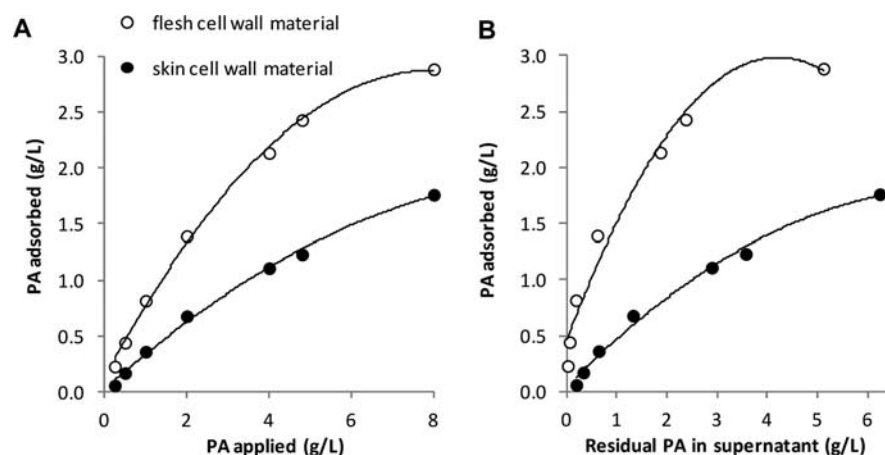


**Figure 1.** Adsorption kinetics of a ripe proanthocyanidin (PA) isolate by 10 mg samples of skin and flesh cell wall extracts in 1 mL of solution: (A) adsorption as a function of the concentration of PA added; (B) adsorption as a function of the residual PA in supernatants.

methanol containing 0.05% v/v TFA after each sample. The PA fractions eluted were concentrated under reduced pressure at 35 °C to remove organic solvent, and the aqueous fraction was recovered. The aqueous fraction was frozen at −80 °C and lyophilized to a dry powder. Dried PA isolates were stored in the dark under nitrogen at −20 °C prior to analysis.

**Binding Studies of Proanthocyanidin Isolates to Cell Wall Material.** The binding assay for grape skin and flesh cell wall material with PA isolates was modified from that described previously.<sup>9</sup> Each reaction was performed in triplicate. The concentration of PA was selected to be below saturation for grape cell wall material on the basis of calculated adsorption kinetics for skin and flesh isolates (Figure 1). This was to limit secondary interactions between PAs and allow for selectivity of cell walls for PA molecular size classes to be determined.<sup>5,6</sup> Although the data generated do not reflect the maximum adsorption capacity of each cell wall sample, they allow for a determination of the relative affinities between samples, because the affinity constant of cell wall material for a range of PA concentrations is expected strongly related to  $N_{\max}$ .<sup>5</sup> Flesh and skin cell wall materials were weighed into 1.5 mL centrifuge tubes in 10 mg quantities. Cell wall materials were combined with PA isolates at 2 g/L containing 12% v/v ethanol and 0.01% v/v TFA, in a 1 mL reaction volume, and incubated for 1 h at 27 °C with shaking. For each reaction, a PA standard blank of the respective PA combination without cell wall material was included to account for possible reduction in PA recovery due to self-association, precipitation, or oxidation. Following the binding reaction, samples were centrifuged at 16000g, and a 500  $\mu$ L aliquot of the supernatant was transferred to a new 1.5 mL centrifuge tube. Samples were then dried under vacuum at 35 °C in a Heto vacuum centrifuge (Heto-Holten A/S, Allerød, Denmark). Recovered PA was then reconstituted in 100  $\mu$ L of methanol and analyzed by phloroglucinolysis and GPC as described below.

**Acid Catalysis in the Presence of Excess Phloroglucinol (Phloroglucinolysis).** Skin PA isolates and PAs recovered from the binding reactions were characterized by phloroglucinolysis<sup>18</sup> to determine the change in PA concentration in supernatants following adsorption, with the high-throughput adaptation followed.<sup>2,8</sup> The phloroglucinolysis reaction was carried out at 50 °C for 25 min, neutralized, and analyzed by RP-HPLC according to the conditions outlined in the original method<sup>18</sup> using (−)-epicatechin (Sigma-Aldrich, St. Louis, MO, USA) as the quantitative standard.

**Gel Permeation Chromatography.** The GPC method was adapted from that previously described<sup>7</sup> to allow for increased size distribution resolution of high molecular mass PAs.<sup>9</sup> The 100 Å column described in the original method was replaced by a 300  $\times$  7.5 mm, 5  $\mu$ m, 10<sup>4</sup> Å column (Varian Inc., Mulgrave, VIC, Australia). The column arrangement and chromatographic conditions were the same as in the original method. The pre-irradiation skin PA fractions of known

mDP (by phloroglucinolysis) used as standards for calibration were the same as previously described.<sup>8</sup> For calibration, a second-order polynomial was fitted with the PA elution time at 50% for each standard. For GPC analysis, PA samples in methanol were diluted with 4 volumes of the HPLC mobile phase. The maximum amount of PA injected onto the column was 40  $\mu$ g.

**Monosaccharide Composition and Klason Lignin in Cell Wall Isolates.** Cell wall samples with distinct binding properties for PAs were selected for compositional analysis. Analyses were in duplicate. Total cell wall polysaccharides (monosaccharides and cellulosic glucose) and acid-insoluble residue (Klason lignin) were estimated according to the hydrolysis procedure using H<sub>2</sub>SO<sub>4</sub> outlined in ref 19. For the analysis of hydrolytically released monosaccharides and cellulosic glucose, respectively, an adaptation of the method of ref 20 was used. Hydrolysates were adjusted to 0.3 M NaOH, combined 1:1 (v/v) with 0.5 M methanolic 1-phenyl-3-methyl-5-pyrazolone (PMP) (Sigma-Aldrich), and heated at 70 °C for 1 h. Samples were cooled and neutralized with 0.3 N HCl, and the excess PMP was extracted three times in diethyl ether. The aqueous fraction retained was then dried under vacuum at 30 °C in a Heto vacuum centrifuge (Heto-Holten A/S). The sample was then resuspended in Milli-Q water to approximate a loading for HPLC of 1 nmol of monosaccharides per 10  $\mu$ L injection.

PMP-monosaccharide derivatives were quantified by HPLC using a C18 column (Kinetex, 2.6  $\mu$ m, 100 Å, 100  $\times$  3.0 mm) protected with a guard cartridge (KrudKatcher Ultra HPLC in-line filter, 0.5  $\mu$ m) (Phenomenex, Lane Cove, NSW, Australia). The mobile phases were solvent A, 10% (v/v) acetonitrile in 40 mM aqueous ammonium acetate, and solvent B, 70% (v/v) acetonitrile in water. The following linear gradient was used: for solvent A (with solvent B making up the remainder) 92% at 0 min; 84% at 12 min; to 0% at 12.5 min; 0% at 14 min, then returning to the starting conditions at 14.5–18.5 min, 92%. A flow rate of 0.6 mL/min was used with a column temperature of 30 °C. The PMP-monosaccharide derivatives were identified according to the retention times of commercial standards (Sigma-Aldrich).

**Uronic Acids in Cell Wall Materials.** The uronic acid content was determined colorimetrically, in duplicate samples, using D-galacturonic acid as the standard.<sup>21</sup> Because flesh contains higher relative concentrations of soluble polysaccharides,<sup>17</sup> the cell wall extraction protocols differed for the skin and flesh tissues, with flesh undergoing pre-extraction in aqueous buffer. Due to possible differences in the respective cell wall isolation procedures, isolated skin cell wall material from different ripeness stages was compared before and after exhaustive extraction with Milli-Q water. Uronic acids were selected as a marker for soluble polysaccharide, as these are expected to be present in the highest concentration relative to other monosaccharides.<sup>13</sup> It was found that the concentration of uronic acids did not decrease following the water extraction, nor did the observed ripening profile in uronic acids change (data not shown). It was therefore



**Table 1. Developmental Changes in Grape Berry Composition and Gravimetric Recovery of Skin and Flesh Cell Wall Material from Preveraison (Green) Onward for the 2009 and 2010 Seasons<sup>a</sup>**

sampling date	days after veraison <sup>b</sup>	juice soluble solids (°Brix)	berry wt (g/berry)	juice content (mL/berry)	cell wall material	
					flesh <sup>c</sup> (mg/berry)	skin <sup>d</sup> (mg/berry)
2009 season						
January 9 <sup>e</sup>	-11	nd <sup>f</sup>	0.54 ± 0.01	nd	2.2 ± 0.52	10.4 ± 0.26
February 23	34	22.4	0.89 ± 0.01	0.46 ± 0.01	3.4 ± 0.16	10.7 ± 0.15
March 2	41	23.4	0.92 ± 0.06	0.45 ± 0.06	3.5 ± 0.58	12.6 ± 1.59
March 26	65	25.8	1.02 ± 0.02	0.53 ± 0.01	4.1 ± 0.33	15.9 ± 0.38
2010 season						
January 15 <sup>e</sup>	-11	nd	0.53 ± 0.03	nd	2.7 ± 0.25	8.0 ± 0.57
January 26 <sup>g</sup>	0	13.2	0.86 ± 0.03	0.46 ± 0.05	2.4 ± 0.11	11.1 ± 0.28
February 9	14	18.0	0.92 ± 0.02	0.50 ± 0.02	2.4 ± 0.27	10.7 ± 0.20
February 16	21	19.8	0.98 ± 0.02	0.52 ± 0.02	2.6 ± 0.13	10.9 ± 0.17
February 23	28	21.7	1.02 ± 0.01	0.51 ± 0.02	2.7 ± 0.13	11.9 ± 0.47
March 2	35	23.8	0.99 ± 0.03	0.52 ± 0.03	2.4 ± 0.13	12.4 ± 0.16
March 10	43	24.0	0.99 ± 0.01	0.52 ± 0.01	3.1 ± 0.19	12.2 ± 0.11
March 17	50	26.1	1.07 ± 0.04	0.54 ± 0.02	3.3 ± 0.09	13.6 ± 0.20

<sup>a</sup>*n* = 3, mean ± SE of the mean. <sup>b</sup>The 2009 or 2010 calculated days after veraison according to Table 1. <sup>c</sup>Gravimetric recovery of dry flesh cell wall material following sequential extraction in 70% (v/v) acetone and buffered phenol. <sup>d</sup>Gravimetric recovery of dry skin cell wall material following extraction in 70% (v/v) acetone, where loss by mass with phenol extraction was <2%. <sup>e</sup>Pre-veraison (green) berry development stage. <sup>f</sup>nd, not determined. <sup>g</sup>Veraison berry development stage designates onset of ripening.

concluded that differences between skin and flesh insoluble cell wall composition due to the extraction protocol followed were minimal.

**Cell Wall Linkage Analysis.** Linkage analysis of the glycosyl residues was determined following methylation with CH<sub>3</sub>I/NaOH according to published methods in duplicate samples.<sup>22,23</sup> Partially methylated alditol acetates were analyzed by GC-MS on a BPX70 capillary column (SGE, Ringwood, VIC, Australia) and identified on the basis of their retention times and fragmentation patterns.<sup>24,25</sup> Assignment of derived linkages were as follows: 1,5-arabinofuranose was assigned to arabinan; 1,2,3,4-galactopyranose, 1,4-galactopyranose, 1,3,4-galactopyranose, and terminal arabinofuranose (equal to 1,3,4-galactopyranose) were assigned to arabinogalactan I; and 1,3-galactopyranose, 1,3,6-galactopyranose, and terminal arabinofuranose (equal to 1,3,6-galactopyranose) were assigned to arabinogalactan II; 1,4-mannopyranose, 1,4,6-mannopyranose, and terminal galactopyranose (equal to 1,4,6-mannopyranose) were assigned to heteromannan (galactomannan); 1,4,6-glucopyranose, 1,4-glucopyranose (equal to 1,4,6-glucopyranose), terminal xylopyranose, terminal fucopyranose, and terminal galactopyranose were assigned to xyloglucan; 1,4-xylopyranose, 1,2,4-xylopyranose, 1,2,3,4-xylopyranose, and terminal arabinofuranose (equal molar proportion to 1,2,4-xylopyranose and 2 molar quantity of 1,2,3,4-xylopyranose) were assigned to heteroxylan (glucuronarabinoxylan). The remaining 1,4-glucopyranose was assigned to cellulose.

**Elemental Composition of Cell Wall Isolates.** Analysis of the non-nitrogen elemental composition and total nitrogen of the cell wall material was determined by inductively coupled plasma atomic absorption spectroscopy (ICPOES) and by the combustion technique, respectively, by an external provider (Waite Analytical Services, School of Agriculture and Wine, University of Adelaide, Australia). Sample measurements were integrated in duplicate. Standard reference fiber materials were included in the batch analysis to determine the reproducibility of the measurement. For the ICPOES method the percentage standard deviation was <7.5% for all detectable elements, and for nitrogen analysis this was <1.5%. Total crude protein of the cell wall samples was determined by multiplying the nitrogen value by 5.27, calculated using previously published data for grape cell wall amino acid composition.<sup>13</sup>

**Direct Phloroglucinolysis on Cell Wall Materials.** Insoluble, cell wall bound PA was determined by direct phloroglucinolysis using an adaptation of a previously published method.<sup>3</sup> Analyses were performed in duplicate. A 50 mg sample of cell walls was placed in a 12 mL test tube, covered with 2 mL of a methanol solution containing 0.1

N HCl, 50 g/L phloroglucinol, and 10 g/L ascorbic acid, and sealed. The reaction was performed in a water bath equipped with a shaker for 25 min at 50 °C. After incubation, the reactions were stopped on ice, neutralized with sodium acetate, and stirred. An aliquot of the supernatant was removed, centrifuged at 16000g for 10 min, and then analyzed by HPLC as described above.

**Statistical Analysis.** Within-season significant differences in PA binding response between tissue type and ripeness levels were determined from triplicate experiments with one-way analysis of variance (ANOVA) using the JMP 5.0.1 statistical software package (SAS, Cary, NC, USA). ANOVAs were followed by a post hoc Tukey's HSD test to determine differences between treatment means. Principal component analysis (PCA) and principal component regression analysis (PCR) were performed using The Unscrambler 10.1 software (CAMO Software AS, Oslo, Norway) using full cross validation. Linear regression analysis was performed using Microsoft Excel 2007 software.

## RESULTS AND DISCUSSION

**Overview of Grape Berry Development.** Berry samples were collected over two seasons at different developmental stages from preveraison (green) to a total soluble solids ripeness of approximately 26 °Brix. In both seasons berry weight and juice volume per berry reached a maximum early during ripening (Table 1) and increased marginally as soluble solids accumulated. Gravimetrically recovered quantities of cell wall material from skin and flesh were similar for the two seasons studied. Gravimetrically recovered skin cell wall material was consistently higher than flesh cell wall material throughout grape berry ripening. In general, cell wall material per berry increased from the earliest to the latest sampling points in grape development.

**Compositional Characteristics of Proanthocyanidins.** To study PA adsorption characteristics, cell wall materials were incubated with two purified PAs from preveraison (green) and ripe grape skins. Both were from Cabernet Sauvignon in the 2009 season, and a detailed analysis of the reaction of these extracts with cell wall material has been previously published.<sup>9</sup> Characteristics of the PAs were determined by their relative subunit composition using the phloroglucinolysis method (Table 2) and GPC (Figure 2). The GPC traces overlaying

Table 2. Subunit Composition of Proanthocyanidin Extracts from Preveraison and Ripe Cabernet Sauvignon Grape Skins

proanthocyanidin source	MC <sup>b</sup> (%)	mDP <sup>c</sup>	MM <sup>d</sup> (subunit)	MM <sup>e</sup> (GPC 50%)	terminal subunits <sup>a</sup>			extension subunits <sup>a</sup>		
					C	E	ECG	EGC-P	(C+E)-P	ECG-P
preveraison	84.9	17.8	5365	4440	91.1	5.4	3.6	60.9	36.4	2.7
ripe	69.2	33.1	10039	9477	74.0	23.5	2.5	63.0	34.1	2.9

<sup>a</sup>Percent composition of proanthocyanidin subunits (in moles) with the following subunit abbreviations: (-P), phloroglucinol adduct of extension subunit; EGC, (-)-epigallocatechin; C, (+)-catechin; EC, (-)-epicatechin; ECG, (-)-epicatechin-3-O-gallate. <sup>b</sup>Mass conversion based on percent recovery of proanthocyanidin by phloroglucinolysis based on the gravimetric mass. <sup>c</sup>Mean degree of polymerization in epicatechin units. <sup>d</sup>Molecular mass as determined by phloroglucinolysis. <sup>e</sup>Molecular mass as determined by GPC at 50% proanthocyanidin elution.

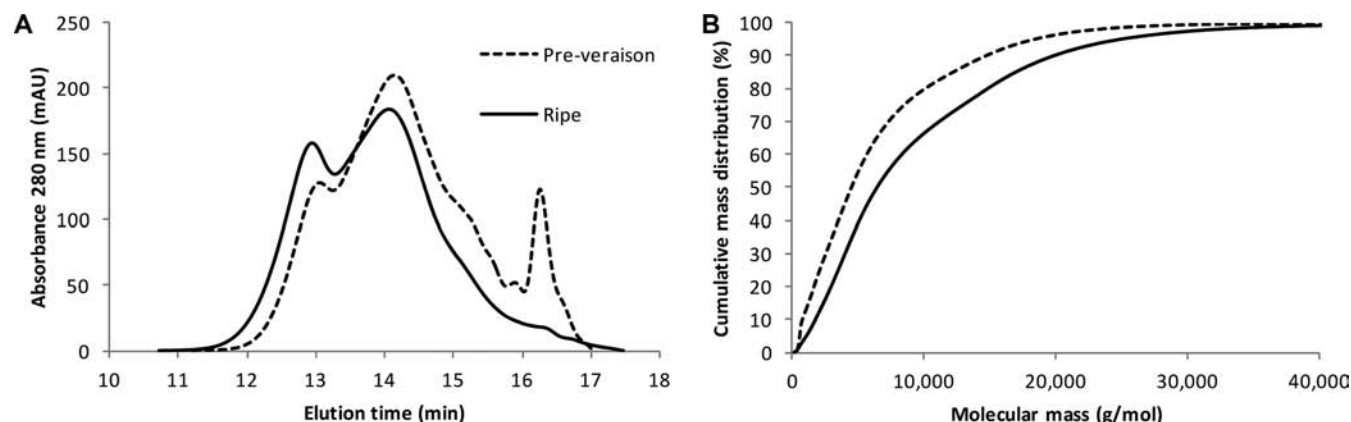


Figure 2. Molecular mass distribution of proanthocyanidins sourced from preveraison and ripe Cabernet Sauvignon grape skins used to determine the adsorption properties of cell wall materials: (A) elution profile; (B) cumulative mass distribution determined by gel permeation chromatography.

Table 3. Adsorption of Two Characterized Preveraison and Ripe Grape Skin PAs by Flesh and Skin Cell Wall Material from Different Developmental Stages in the 2009 and 2010 Seasons

sampling date	days after veraison <sup>b</sup>	proanthocyanidin adsorption <sup>a</sup> (mg/g cell wall material)			
		preveraison proanthocyanidin		ripe proanthocyanidin	
		flesh	skin	flesh	skin
2009 season					
January 9	-11	126 ± 0.92a	53 ± 2.61d	146 ± 0.19a	55 ± 4.64c
February 23	34	123 ± 1.02a	63 ± 3.05cd	143 ± 1.97a	55 ± 1.05c
March 2	41	129 ± 1.76a	73 ± 2.40bc	147 ± 0.91a	71 ± 3.85b
March 26	65	124 ± 0.40a	76 ± 2.54b	138 ± 1.34a	78 ± 4.76b
2010 season					
January 15	-11	116 ± 2.64c	54 ± 1.45d	146 ± 0.45b	85 ± 4.37c
January 26	0	117 ± 2.38c	22 ± 1.49g	161 ± 1.09a	47 ± 4.1f
February 9	14	127 ± 3.86a	29 ± 3.14f	161 ± 0.60a	53 ± 2.64ef
February 16	21	131 ± 1.13ab	33 ± 2.01ef	163 ± 1.18a	62 ± 0.78de
February 23	28	126 ± 1.61b	31 ± 0.27ef	164 ± 1.88a	61 ± 1.91e
March 2	35	128 ± 1.57ab	33 ± 0.73ef	168 ± 0.25a	64 ± 1.41de
March 10	43	133 ± 0.29a	36 ± 2.98e	163 ± 0.12a	73 ± 2.70d
March 17	50	120 ± 1.23c	48 ± 0.35d	163 ± 0.52a	94 ± 3.74c

<sup>a</sup>Proanthocyanidins were extracted from pre-veraison and ripe grape skins; each data point is the mean of  $n = 3 \pm SE$ . Data were analyzed using a one-way ANOVA per season  $\times$  proanthocyanidin type treatment;  $P < 0.001$  followed by post-hoc Tukey's HSD test; different letters indicate significant differences within each season  $\times$  proanthocyanidin column. <sup>b</sup>The 2009 or 2010 calculated "days after veraison" according to Table 1.

the elution profile (Figure 2A) and the cumulative mass distribution (Figure 2B) indicate that the PA from ripe grape skins had a higher proportion of high molecular mass material (earlier eluting) of the two PAs. The shift in the elution profile from preveraison to ripe grape skin PAs shows a loss in oligomeric and lower molecular mass material. This was reflected in a net shift of the cumulative mass distribution of the ripe PA to a higher molecular mass at 50% elution. The analysis of the PAs by phloroglucinolysis confirmed the GPC data and indicated that the mDP increased from the

preveraison to the ripe extract. In terms of PA composition, analysis of the ripe extract indicated a loss in the proportion of catechin and epicatechin-3-O-gallate as terminal subunits from the preveraison extract, with proportionally higher epicatechin. For the extension subunits, differences in the proportions of subunit types were negligible between the PA extracts.

**Adsorption of Proanthocyanidin by Skin and Flesh Cell Wall Material.** The adsorption characteristics of isolated cell wall material for the two PAs tested are shown in Table 3 as PA bound per unit cell wall material. The adsorption of PAs by

**Table 4. General Compositional Analysis of Cell Wall Components (in Milligrams per Gram Dry Weight of Grape Flesh and Skin Cell Wall Isolates)**

sampling date <sup>a</sup>	grape berry tissue	total polysaccharides <sup>b</sup>	uronic acids <sup>c</sup>	noncellulosic neutral sugars <sup>d</sup>	cellulose <sup>e</sup>	crude protein <sup>f</sup>	inorganic ions <sup>g</sup>	insoluble proanthocyanidin <sup>h</sup>	Klason lignin <sup>i</sup>
2009 season									
January 9 (-11)	flesh	467	208 (44) <sup>j</sup>	158 (34) <sup>j</sup>	101 (22) <sup>j</sup>	176	15	62	233
March 26 (65)		272	103 (38)	92 (34)	77 (28)	185	57	17	206
January 9 (-11)	skin	379	103 (27)	143 (38)	133 (35)	58	4	166	476
March 2 (41)		290	71 (24)	115 (40)	104 (36)	105	7	82	453
March 26 (65)		283	76 (27)	109 (39)	97 (34)	95	10	101	465
2010 season									
January 15(-11)	flesh	413	187 (45)	119 (29)	107 (26)	178	10	59	294
March 17 (50)		283	71 (25)	105 (37)	107 (38)	229	19	21	168
January 15 (-11)	skin	487	235 (48)	156 (32)	96 (20)	60	6	85	436
January 26 (0)		372	133 (36)	122 (33)	118 (32)	83	8	144	464
February 16 (21)		336	140 (42)	109 (32)	87 (26)	107	9	126	442
March 2 (35)		318	107 (34)	103 (33)	107 (34)	107	11	129	477
March 10 (43)		318	103 (32)	107 (34)	108 (34)	110	10	124	467
March 17 (50)		317	99 (31)	112 (35)	106 (33)	99	13	108	455

<sup>a</sup>Date sample collected; number in parentheses is the 2009 or 2010 "days after veraison" according to Table 1. <sup>b</sup>Total polysaccharide mg/g of the sum of uronic acids, noncellulosic monosaccharides, and cellulose. <sup>c</sup>Uronic acids determined spectrophotometrically as mg/g galacturonic acid units. <sup>d</sup>Monosaccharide determined following mild acid hydrolysis. <sup>e</sup>Cellulosic glucose from harsh acid (Seaman's) hydrolysis as mg/g. <sup>f</sup>Crude protein as mg/g nitrogen  $\times$  5.27. <sup>g</sup>Inorganic ions determined by inductively coupled plasma atomic emission spectrometry as mg/g. <sup>h</sup>Cell-wall bound proanthocyanidin determined by direct phloroglucinolysis as mg/g. <sup>i</sup>Dry weight of acid-insoluble residue of harsh acid (Saeman's) hydrolysis as mg/g; when total recovery of all components exceeds 1 g, this may be due to repolymerization of hydrolyzed proanthocyanidin to this residue. <sup>j</sup>Numbers in parentheses are the percentage of this component of total polysaccharide.

the cell wall isolates was compared separately, because these were previously shown to have unique binding properties for grape cell wall extracts.<sup>9</sup> PA adsorption was consistently lower for skin cell wall material than for flesh cell wall material for both seasons studied, independent of the ripeness stage tested. This finding confirms our previous observations for the two cell wall sources within Shiraz grape tissues<sup>3,8,9</sup>

For the 2009 season, commercially ripe (>23 °Brix) skin cell wall material bound a greater amount of PA compared with the preveraison extract, and this was observed for both PAs tested. In the 2010 sample series, additional samples were included to capture information from the earlier stages of ripening. In the 2010 experiment, the preveraison skin cell wall isolate bound more PA than that isolated at veraison, which was unexpected on the basis of the 2009 observations. However, a significant trend was shown in which PA adsorption by skin cell wall material increased as ripening progressed postveraison, with the final sampling date (50 days after veraison) being equivalent to the preveraison measure.

For flesh cell wall material, PA adsorption properties did not demonstrate ripening-specific changes that were consistent for season and PA type tested. For the 2009 cell wall isolates, PA adsorption did not change significantly with the progression of ripening for either PA type used in the assay. In the 2010 developmental series, adsorption of both PAs by the preveraison cell wall extract was lowest. Using ripe PA in the assay, no significant changes in adsorption by flesh cell wall material were observed from veraison onward. Conversely, adsorption of preveraison PA showed a minor increase in the amount bound at 14 days after veraison, which then remained constant, decreasing in the final ripeness stage sampled. However, by comparison with skin cell wall materials, in which variation in PA adsorption between ripeness stages was ~30% in 2009 and ~60% in 2010, variation in the PA-binding response of flesh cell wall materials was minor (~13%).

#### Multivariate Analysis of Cell Wall Composition and Proanthocyanidin Adsorption Properties.

A broad compositional analysis of cell wall samples selected from the PA adsorption study, which had demonstrated distinct binding properties for PAs, was conducted (Tables 4 and 5). An exploratory PCA of the data set (data not shown) was followed by a PCR analysis (Figure 3) to determine whether a model could be developed to explain the adsorption of grape skin PAs based on cell wall composition. The PCR variance (>90%) was maximally explained using two principal components (PCs), shown in Figure 3. The data were well-modeled by the PCR analysis, which revealed differences between skin and flesh cell wall adsorption of PA in PC1 (Figure 3). The inclusion of PC2 allowed for differences in ripeness to be described.

According to the model indicators as defined by PC1, key differences in cell wall composition between flesh and skin that are related to adsorption properties for PA are linked to lower acid-insoluble fiber, cell wall mannose, and insoluble PA in the former, with concomitantly higher wall-bound (crude) protein, inorganic ions (primarily potassium), and cell wall rhamnose. However, due to the very low molar proportion of mannose and rhamnose in cell wall polysaccharides (Table 5), it is unlikely that these changes could confer significant structural modification of the cell wall.

Changes in cell wall properties with ripening were poorly defined by PC1. A review of the compositional data that defined this principal component (Table 4; Supporting Information S1) showed that, generally, flesh cell wall material had reduced acid-insoluble fiber in ripe samples relative to the preveraison measure, but this effect was not observed in skin samples, where the acid-insoluble fraction remained high (>45% w/w) regardless of the ripening stage. Additionally, ripening grapes had lower insoluble PA in cell walls than the preveraison measure, although for skin cell walls in the 2010 sample set this was highest at veraison. Ripening grapes also had small increases in cell wall-bound protein and inorganic

Table 5. Composition of Monosaccharides (as Millimoles per Gram and Molar Proportion in Dry Flesh and Skin Cell Wall Material Samples)

sampling date <sup>a</sup>	grape berry tissue	mannose <sup>b</sup>	rhamnose <sup>b</sup>	uronic acids <sup>c</sup>	glucose (noncellulosic) <sup>b</sup>	glucose (cellulosic) <sup>d</sup>	galactose <sup>b</sup>	xylose <sup>b</sup>	arabinose <sup>b</sup>	fucose <sup>b</sup>
2009 season										
January 9 (-11)	flesh	27.3 (1)	39.4 (1.5)	1071.3 (41.2)	134.7 (5.2)	563.1 (21.7)	246.0 (9.5)	189.7 (7.3)	286.0 (11)	40.5 (1.6)
March 26 (65)		20.5 (1.3)	36.7 (2.4)	529.7 (34.4)	46.4 (3)	427.4 (27.8)	73.3 (4.8)	108.5 (7.1)	275.2 (17.9)	20.0 (1.3)
January 9 (-11)	skin	42.8 (2)	23.6 (1.1)	530.1 (24.9)	52.1 (2.4)	736.4 (34.5)	322.3 (15.1)	130.5 (6.1)	270.7 (12.7)	24.5 (1.1)
March 2 (41)		36.1 (2.2)	28.0 (1.7)	363.3 (22)	92.0 (5.6)	575.5 (34.8)	111.9 (6.8)	115.7 (7)	308.5 (18.6)	23.6 (1.4)
March 26 (65)		32.3 (2)	27.4 (1.7)	393.4 (24.4)	106.3 (6.6)	538.6 (33.5)	82.3 (5.1)	110.2 (6.8)	293.3 (18.2)	26.0 (1.6)
2010 season										
January 15 (-11)	flesh	22.5 (1)	39.2 (1.7)	961.6 (42)	57.2 (2.5)	595.7 (26)	181 (7.9)	166.6 (7.3)	231.8 (10.1)	35.5 (1.5)
March 17 (50)		23.5 (1.4)	43.2 (2.7)	368.2 (22.7)	47.8 (2.9)	593.4 (36.5)	78.4 (4.8)	137.7 (8.5)	304.5 (18.8)	27.3 (1.7)
January 15 (-11)	skin	49.1 (1.8)	36.6 (1.4)	1212.5 (45.1)	47.4 (1.8)	532 (19.8)	320.3 (11.9)	159.5 (5.9)	298.5 (11.1)	34.5 (1.3)
January 26 (0)		39.9 (1.9)	29.4 (1.4)	682.6 (32.8)	44.4 (2.1)	654.5 (31.4)	210.9 (10.1)	131.7 (6.3)	262.9 (12.6)	27.2 (1.3)
February 16 (21)		36.8 (2.0)	30.7 (1.6)	719.1 (38.3)	65.3 (3.5)	483.5 (25.7)	128.9 (6.9)	113.7 (6.1)	276.4 (14.7)	23.6 (1.3)
March 2 (35)		30 (1.7)	27.9 (1.6)	551.3 (30.8)	76 (4.3)	595 (33.3)	103.7 (5.8)	104.4 (5.8)	273.9 (15.3)	25.3 (1.4)
March 10 (43)		32.3 (1.8)	30.1 (1.7)	528.7 (29.4)	78.7 (4.4)	600.7 (33.5)	104.1 (5.8)	112.1 (6.2)	284.7 (15.9)	23.7 (1.3)
March 17 (50)		33.5 (1.9)	29.8 (1.7)	507.4 (28.3)	91.7 (5.1)	589.4 (32.8)	105.3 (5.9)	112.3 (6.3)	300.3 (16.7)	24.7 (1.4)

<sup>a</sup>Date sample collected; number in parentheses is the 2009 or 2010 "days after veraison" according to Table 1. <sup>b</sup>Monosaccharide determined following mild acid hydrolysis presented as  $\mu\text{mol/g}$  dry cell wall material, number in parentheses is the mol % of total polysaccharide. <sup>c</sup>Uronic acids determined spectrophotometrically as galacturonic acid units  $\mu\text{mol/gdry}$  cell wall material. <sup>d</sup>Cellulosic glucose from harsh acid (Saeman's) hydrolysis as  $\mu\text{mol/gdry}$  cell wall material.

ions for both skin and flesh samples, which may explain the partial separation of samples by ripeness on PC1. An analysis of insoluble PA molecular mass by direct phloroglucinolysis showed that it increased as ripening progressed, up to 30% in flesh cell walls and 54% in skin cell walls (Supporting Information S2). Because the phloroglucinolysis method is dependent upon resolution of PA subunits as terminal and extension units, this increase in molecular mass may result from a loss in recovered terminal units. The possibility that covalent linkages between PA units and cell wall residues could occur in situ during grape development, resulting in a decreased recovery using phloroglucinolysis, cannot be ruled out.

Ripening-related changes in cell wall composition described by PC2 were associated with a loss in total polysaccharide, primarily due to decreasing cell wall galactose, fucose, xylose, and uronic acid contents. Decreases in uronic acids would be presumed to be principally as pectic galacturonic acid because glucuronic acid is a minor component of grape cell walls.<sup>12</sup> Quantitatively, the decrease in polysaccharide was driven primarily by the decrease in galactose and galacturonic acid, with losses in fucose and xylose being minor (Figure 3; Table 5). Losses in polysaccharides during ripening were strongly related to increases in boron in cell wall material. Examination of the data indicated that this occurred for all samples except skin cell wall material from the 2010 ripening series, in which boron remained unchanged by unit mass. However, for all samples, the fucose/boron ratio decreased with ripening (Table 5; Supporting Information S1).

Linkage analysis was performed on selected samples to confirm whether observed changes in monosaccharide composition were related to structural changes within the neutral polysaccharide fraction or could provide additional insights overlooked by the broader compositional analysis. The observed loss in galactose from the skin cell walls during ripening was confirmed by linkage analysis to be primarily due to a loss in arabinogalactan I polysaccharides (Figure 4A; Supporting Information S3), as changes in arabinogalactan II were negligible. Similarly, for flesh cell wall samples analyzed from both seasons, the loss in arabinogalactan I was quantitatively the most significant during ripening. For other neutral cell wall polysaccharides in skin cell walls, significant changes in composition by linkage analysis were not observed during ripening (Figure 4B).

The proportion of cellulose in ripening skin cell walls determined by linkage analysis was smaller than that determined by difference using differential (mild and then harsh)  $\text{H}_2\text{SO}_4$  hydrolysis. However, as changes in cellulose (by both methods) were found to be minor during ripening and between cell walls of different origin in the grape berry, this methodological difference was not pursued further. In general, the compositional polysaccharide changes observed for cell walls during ripening were similar for skin and flesh, and changes following the pre-ripening period were minimal. As such, these could not be used to define the observed differences in PA adsorption properties.

**Nonpolysaccharide Cell Wall Components.** In observing the large difference in PA adsorption between flesh and skin cell wall materials in this study on Cabernet Sauvignon, we have noted this previously in another grape cultivar, Shiraz.<sup>3,8,9</sup> These previous studies, which looked at crude characterization of Shiraz cell wall fractions by comparing their relative solubility in neutral or acid detergents,<sup>3,26,27</sup> concluded that a key difference between the materials was that the estimated lignin,



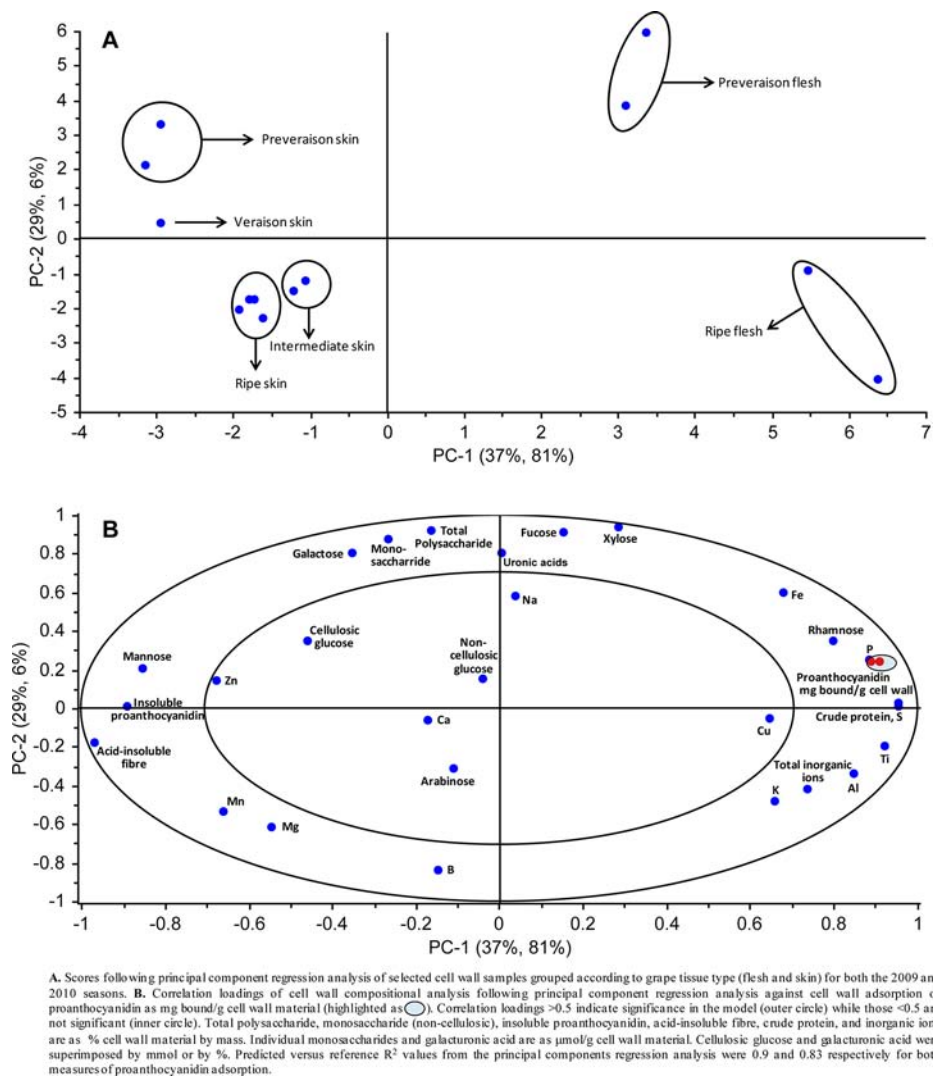


**Figure 3.** Principal component regression analysis showing (A) scores and (B) correlation loadings of cell wall compositional attributes as they relate to the adsorption of two grape skin proanthocyanidins (preveraison and ripe) by cell walls from different grape tissues, seasons, and ripeness stages.

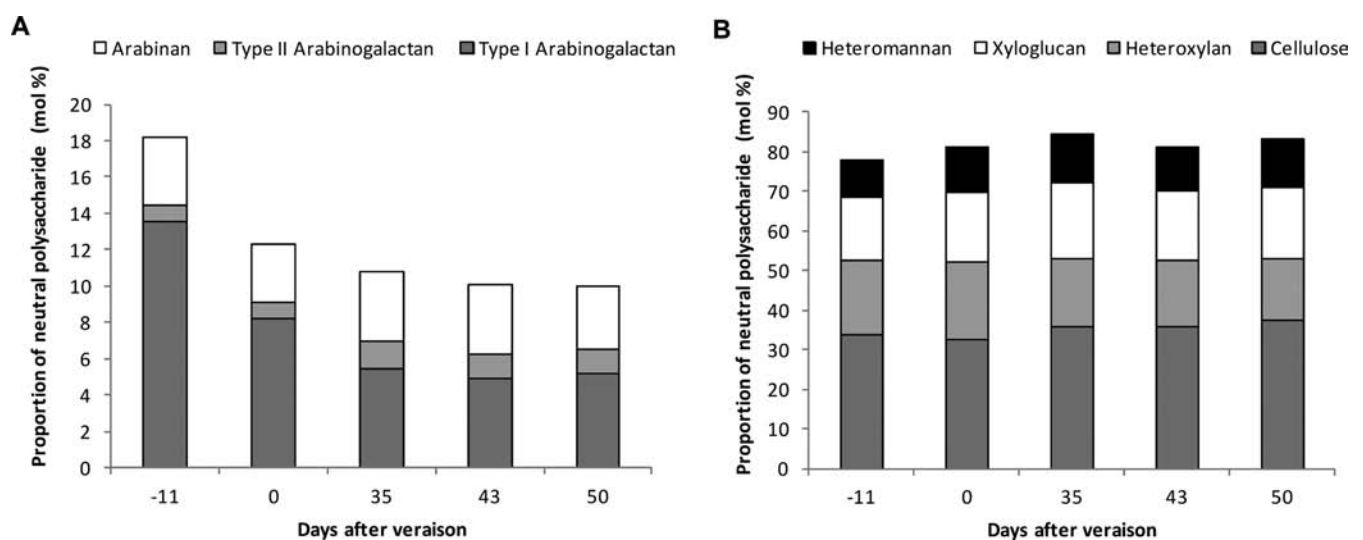


**Figure 4.** Linkage analysis of neutral skin cell wall polysaccharides from the 2010 developmental series; (A) pectic polysaccharide side chains arabinan, arabinogalactan I, and arabinogalactan II; (B) noncellulosic polysaccharides and cellulose.



**Table 6. Linear Regression Equations Derived from the Percentage Change by Molecular Mass Category of Preveraison and Ripe Proanthocyanidins before and after Adsorption by Ripening Skin Cell Wall Samples for the 2010 Season**

elution slice <sup>a</sup> (%)	preveraison skin proanthocyanidin			ripe skin proanthocyanidin		
	MM av <sup>b</sup>	regression eq <sup>c</sup>	R <sup>2</sup>	MM av <sup>b</sup>	regression eq <sup>c</sup>	R <sup>2</sup>
10	802	$y = 1.22x - 0.04$	0.82	1860	$y = 1.65x - 6.21$	0.81
30	2573	$y = 2.41x - 12.77$	0.75	4110	$y = 1.69x - 2.89$	0.80
50	4516	$y = 1.85x - 11.90$	0.72	6583	$y = 2.63x - 4.55$	0.87
70	7326	$y = 2.92x - 17.45$	0.78	11494	$y = 4.88x - 13.56$	0.90
90	14684	$y = 6.14x - 36.8$	0.84	20527	$y = 4.35x - 14.6$	0.87

<sup>a</sup>Cutoff points (slices) determined as a percentage elution of the whole proanthocyanidin isolate as a function of time. <sup>b</sup>Data represent the average molecular mass (MM) average for each MM category determined by cumulative elution using gel permeation chromatography. An elution of 10% is the smallest proanthocyanidin MM and 90% largest MM calculated for a sample. <sup>c</sup>Regression equations were derived from veraison and ripening skin cell wall samples for 2010 only.

cellulose, and insoluble PA content in skin cell walls was higher, while neutral-detergent soluble material (pectin, proteins) was lower. It was proposed that these compositional characteristics might impart a reduced flexibility and porosity to the cell wall matrix. In the current study the yield of acid-insoluble fiber (lignin) was higher than previously reported.<sup>3</sup> The Shiraz skin and flesh materials previously analyzed using the detergent fractionation method<sup>3,26,27</sup> were subjected to the same analyses as reported in the current study, and the yield of acid-insoluble fiber was consistent with the results for the Cabernet Sauvignon cell wall samples (unpublished data). This indicates that the method applied rather than the sample composition determines the high yields of acid-insoluble fiber for grape cell walls. Reports compared the two methods for lignin analysis, and it has been proposed that the acid hydrolysis methods have a higher accuracy for lignin recovery, but may be compromised by contamination of the material with a high content of insoluble PA.<sup>28</sup> By comparison with other nonvascular tissues in dicotyledonous plant species, the estimated Klason lignin is too high, considering that a developed secondary cell wall has not been reported for these tissues apart from the vasculature, which is expected to be a minor component. This may point to interference from insoluble PA in the Klason lignin estimate, in addition to that estimated using the direct phloroglucinolysis technique.

In this study we have demonstrated the presence of a significant proportion of insoluble PA (by dilute acid hydrolysis) in cell wall material using direct phloroglucinolysis. It is well-known that using the phloroglucinolysis method yields incomplete conversion of the PA molecule, which decreases with grape ripening most likely due to inter- and intramolecular PA reaction and/or incorporation of non-PA material into the polymer.<sup>1-3,9,18</sup> Only a proportion of the PA in the cell wall materials, in particular skin cell walls, is therefore measurable using phloroglucinolysis and likely contributes to an over-estimation of the Klason lignin fraction. The observed decrease in insoluble PA in cell walls with ripening, with the concomitant increase in PA molecular mass (Supporting Information S2), may indicate that covalent linkages of PA terminal units have occurred within the cell wall matrix. The concept of a significant PA fraction being incorporated into fiber has been mentioned before,<sup>28</sup> and significant nonextractable PA (27% DW) has been reported in fibers isolated from grape pomace using Porter's assay.<sup>29-31</sup> PAs may become covalently associated into cell walls as tissues are macerated during sample processing, possibly as a result of PA oxidation. Additionally, the possibility that PA may be deposited in cell walls in situ during development should not be overlooked.

Grape PA subcellular distribution is not restricted solely to the vacuole, and a significant fraction of highly polymerized materials is found to be associated with cell wall material.<sup>2,32</sup> The progression of ripening in grape skins is associated with a shift from stored PA within the vacuole to cell wall-associated PA.<sup>32</sup> In other plant species this process has been proposed to be mediated by vesicle trafficking, whereby PAs contained in vesicles are transported from the vacuole to the plasma membrane and then exocytosed into the cell wall, where they are covalently integrated.<sup>33</sup>

The results of the current study show that two of the key structural factors which increase the adsorption of PA in cell walls are the decreases in acid-insoluble fiber and insoluble PA, confirming previous results<sup>3</sup> and pointing to differences in the intrinsic ability of the cell wall network to encapsulate PAs either within pores or within a flexible, folded three-dimensional structure.

A further significant factor that was related to an increase in the adsorption of PA was the increase in crude protein. Crude protein within cell walls is usually reported to be low (<10%) using Lowry's assay or amino acid analysis<sup>13,14</sup> and higher protein contents presumed to be due to contamination of cytoplasmic material. A comparison of cell wall preparation methods has revealed that the use of buffered phenol does not completely extract cytoplasmic proteins, but does reduce this contamination more effectively than other methods.<sup>34</sup> A comparison with ref 17, in which a similar buffered phenol washing method was employed, revealed similar concentrations of protein (also derived from nitrogen analyses) between skin and flesh cell walls, thus suggesting that the high protein values obtained in this study are not simply an artifact of extraction. The possibility that cell wall-bound proteins, in particular, the hydroxyproline-rich glycoproteins which accumulate in cell walls during ripening, can strongly adsorb PAs has been suggested previously.<sup>15</sup> This factor may significantly contribute to the differences in the adsorption of PA between the two tissue types.

**Selectivity of Cell Walls for Proanthocyanidins According to Their Molecular Mass.** Ripening-related modification of cell wall composition did not show a strong relationship to adsorption properties for heterogeneous PA isolates according to multivariate statistical analysis. Hence, we used GPC to explore whether differences in net PA adsorption were conferred by changes in selectivity for PAs according to their molecular mass. This is an important consideration, as strong evidence exists that cell walls vary in their ability to bind PA. Grape flesh cell walls consistently bind higher molecular mass PAs, whereas skin cell walls show a poor capacity to

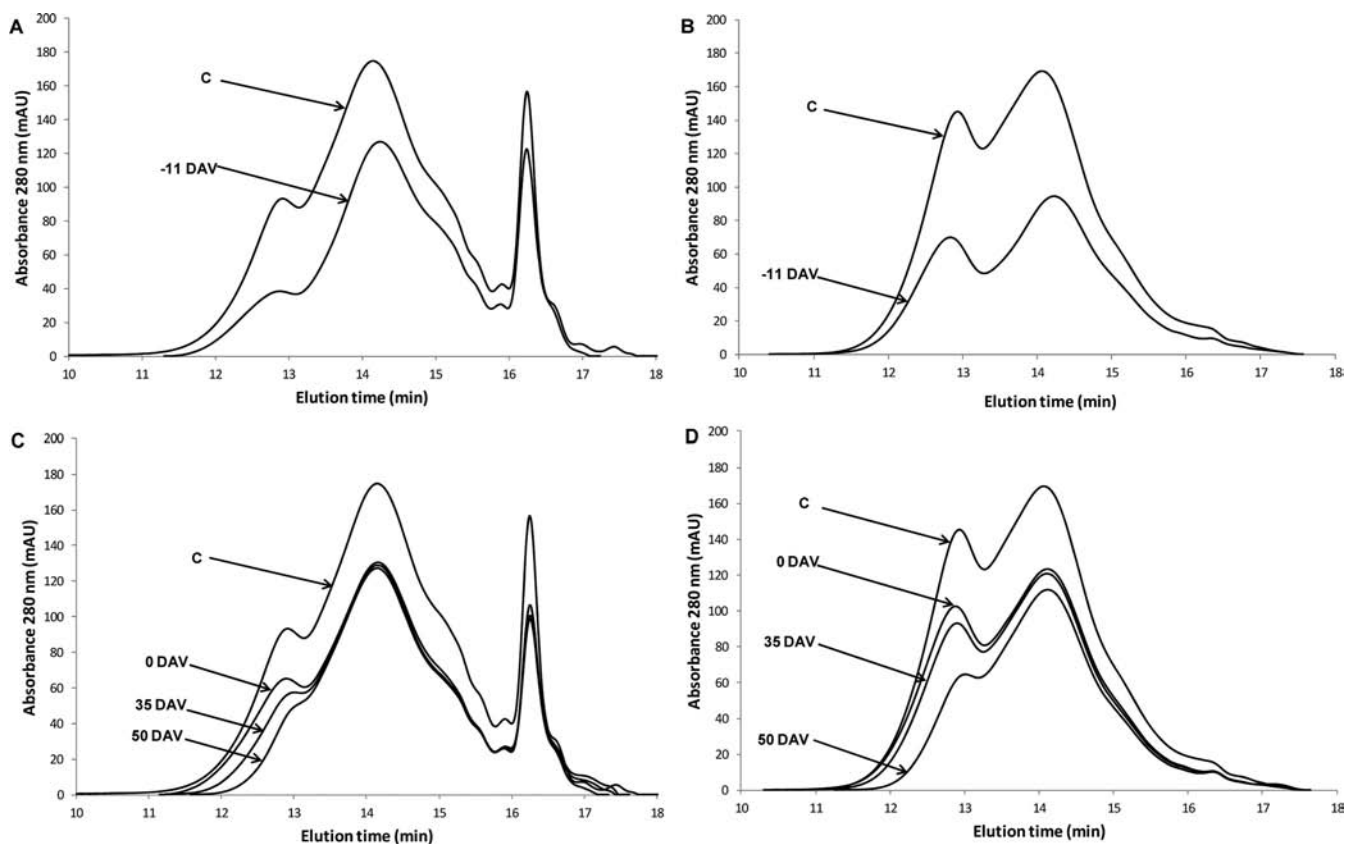


**Figure 5.** Elution profile of PA molecular mass distribution of preveraison and ripe PA before and after reaction with skin cell wall material from different developmental stages in the 2010 season: (A) preveraison PA and (B) ripe PA reacted with preveraison skin cell wall material; (C) preveraison PA and (D) ripe PA reacted with postveraison skin cell wall material. Developmental stages of cell wall samples for the 2010 season are according to Table 1. DAV, days after veraison; C, proanthocyanidin control.

adsorb highly polymerized PAs.<sup>3,9</sup> For flesh cell wall material, the adsorption of PAs was consistent with the loss of higher molecular mass material (Supporting Information S4), whereas oligomers were poorly adsorbed. When a slight increase in flesh cell wall adsorption of PA with the progression of ripening was observed for the 2010 samples (Table 3), this did not change the pattern of selectivity, but enhanced binding of all PA molecular sizes occurred, although for oligomeric PA material this remained low.

For skin cell wall material, the 2010 preveraison cell walls were proportionally richer in galacturonic acid and arabinogalactan I (Tables 5 and 6; Figure 4) and had a PA adsorption response different from skin cell wall isolate samples from ripe grapes. For the preveraison skin cell wall isolate, preveraison PA was selectively removed in the high molecular mass range. Conversely, high molecular mass ripe PA was poorly adsorbed (Figure 5A,B). This effect has been previously reported for grape skin cell wall material and is thought to be dependent on the modification of PA structure with ripening.<sup>3,9</sup> The onset of veraison was characterized by a loss in the adsorption of high molecular mass PAs for both PA types tested. However, with the progression of ripening, skin cell wall isolates showed enhanced selectivity for higher molecular mass PAs, although this effect was more significant for PA from ripe skin (Figure 5C,D). This is most likely due to the PA containing a greater proportion of high molecular mass material (Figure 1). These data indicate that the observed increase in adsorption of PA by skin cell walls with the progression of ripening after veraison was primarily due to increased binding of higher molecular

mass PA. The difference in the reaction of the 2010 preveraison skin cell wall material to the other skin cell wall fractions was that higher molecular mass PA material was preferentially adsorbed from preveraison PAs (Figure 5A). For the reaction with ripe PA extract, on the other hand, PAs of intermediate size were more adsorbed by preveraison than by ripe skin cell walls (Figure 5B).

To confirm the observations using GPC elution profiles, regression analysis of the percentage removal of PAs before and after fining for different molecular mass categories was performed for the 2010 skin cell wall samples (Table 6). The molecular mass categories were determined by GPC and their relative proportions calculated. For the ripening skin cell wall material from veraison onward, there was a positive significant relationship whereby increasing amounts of PA were removed for all PA size categories. This was observed for both PAs tested. The increase in slope for the derived regression equation in the higher molecular mass categories (70 and 90% elution) indicates that adsorption of larger PAs was significantly increased with ripening of the skin cell walls.

For the 2009 skin cell wall samples, preveraison skin cell walls showed a similar response to the 2010 veraison skin cell walls, with poor adsorption of high molecular mass PAs (Supporting Information S5). As for the 2010 ripening series, however, ripe skin cell walls from the 2009 study showed enhanced adsorption of high molecular mass material. Compositional differences between preveraison skin cell walls from 2009 and 2010 were that galacturonic acid was proportionally lower in the 2009 sample (Table 5), indicating

that pectin turnover may have been initiated earlier in that season, yielding PA adsorption properties comparable with the 2010 veraison sample. Because a higher pectin content in cell walls is expected to confer enhanced capacity for PA adsorption,<sup>11</sup> the uniquely high binding capacity of the 2010 preveraison skin cell walls could be explained, in part, by their high pectin content.

This observation reveals a potential shift from a strong surface interaction of PA with galacturonan-rich immature cell walls to a reduced interaction with a weakened, collapsed structure following the turnover of pectin. The continued, although minor, loss of galacturonan and arabinogalactan I in skin cell walls with the progression of ripening is associated with increases in cell wall-bound (glyco)protein. This later increase in (glyco)proteins within grape skin cell walls is known to be associated with accumulation of hydroxyproline-rich extensins.<sup>12,13</sup> The incorporation of these structural proteins is thought to stabilize the cell wall structure, enabling enhanced access of pectin-degrading enzymes. This, in turn, may facilitate an increase in porosity through pectin turnover. The loss of pectins from within the cell wall structure also enables access of cell wall degrading enzymes, notably pectin methyl esterases. In ripening fruits, the sequence of polysaccharide solubilization and depolymerization can vary, as well as the subclass of polysaccharide that undergoes modification.<sup>35</sup> Whereas solubilization of pectic polysaccharides takes place early in grape berry development, depolymerization can take place later.<sup>13</sup> Analysis of the degree of esterification was not undertaken in this study, but other work has shown decreases in the methyl esterification of grape cell walls with ripening, continuing into the later stages of ripening.<sup>13</sup> Availability of de-esterified carboxyl sites on galacturonans usually leads to cross-links via  $\text{Ca}^{2+}$  bridges according to the “egg-box model”. In grape berries,  $\text{Ca}^{2+}$  accumulation in skin and flesh tissues generally ceases at veraison and tends to form crystals within berry structures.<sup>36,37</sup> As such, the primary ion accumulated during ripening is  $\text{K}^+$ , which has been observed to remain soluble, that is, does not form crystals in situ.<sup>36,37</sup> In the current study, this phenomenon is evident in the marked increase in cell wall-bound  $\text{K}^+$  in both flesh and skin cell walls, whereas changes in  $\text{Ca}^{2+}$  were minor. In de-esterified galacturonans, binding by  $\text{K}^+$  can occur in place of  $\text{Ca}^{2+}$ , but does not induce “egg-box” junction zone formation between galacturonans.<sup>38,39</sup> Speculatively, limited gel network formation within the cell wall structure would be expected to contribute to an increase in porosity. Enhanced cell wall porosity may potentially facilitate penetration of large PA molecules within a more open cell wall framework. Increased access of PAs to form hydrogen bonds with polysaccharides and structural proteins within cell wall pores may therefore be associated with skin cell wall ripening.

Nevertheless, we note that in terms of PA adsorption properties during ripening, the response of flesh and skin cell walls differed markedly, despite the observation that changes in cell wall polysaccharides were similar throughout the progression of ripening. As evident from the PA–cell wall interaction results for flesh cell walls, structural modifications similar to those for skin occurred during ripening and did not necessarily induce a difference in PA adsorption characteristics. As proposed in previous work,<sup>3</sup> and again shown in this study, a key structural difference between flesh and skin cell walls may be the limited flexibility and porosity of the latter, which we propose could be conferred by the incorporation of insoluble PA into the cell wall matrix.

The consequences of these findings for processing of grape and wine products is complex. Increased adsorption of PAs to cell walls may restrict their extraction during either vinification or juice production, yet an enhanced porosity may facilitate extraction into hydroalcoholic solutions, in particular, where cell walls are saturated with PA. Future studies will seek to determine the factors that confer adsorption characteristics to cell walls, in particular, those which contribute to either increase or decrease the extractability of PAs under hydroalcoholic conditions.

## ■ ASSOCIATED CONTENT

### 📄 Supporting Information

S1, elemental composition of cell wall material; S2, molecular mass and mDP of insoluble cell-wall bound PAs; S3, arabinogalactan I contribution in skin (2009) and flesh cell wall material (2009 and 2010); S4, PA elution profile after adsorption to preveraison and ripe flesh skin cell walls (2010); S5, PA elution profile after adsorption to preveraison and ripe skin cell walls (2009). This material is available free of charge via the Internet at <http://pubs.acs.org>.

## ■ AUTHOR INFORMATION

### Corresponding Author

\*Phone: +61-8-83136190. Fax: +61-8-83136601. E-mail: [keren.bindon@awri.com.au](mailto:keren.bindon@awri.com.au).

### Funding

The Australian Wine Research Institute, a member of the Wine Innovation Cluster in Adelaide, is supported by Australian grapegrowers and winemakers through their investment body, the Grape and Wine Research and Development Corporation, with matching funds from the Australian government.

### Notes

The authors declare no competing financial interest.

## ■ ACKNOWLEDGMENTS

We thank Orlando-Wyndham Vineyards for the donation of grape samples. We particularly acknowledge Dr. Mike McCarthy of the South Australian Research and Development Institute (SARDI) for access to field trial samples and information. Cherie Therese Walsh, Roshan Cheetamun, and Dr. Jelle Lahnstein from the ARC Centre of Excellence in Plant Cell Walls (University of Melbourne and University of Adelaide, respectively) assisted with technical advice. We thank Fiona Brooks for assistance with grape berry dissection. Finally, we acknowledge Professor Douglas Adams, Dr. Elizabeth Waters, and Dr. Paul Smith for useful discussion.

## ■ REFERENCES

- (1) Kennedy, J. A.; Hayasaka, Y.; Vidal, S.; Waters, E. J.; Jones, G. P. Composition of grape skin proanthocyanidins at different stages of berry development. *J. Agric. Food Chem.* **2001**, *49*, 5348–5355.
- (2) Kennedy, J. A.; Matthews, M. A.; Waterhouse, A. L. Changes in grape seed polyphenols during fruit ripening. *Phytochemistry* **2000**, *55*, 77–85.
- (3) Bindon, K. A.; Smith, P. A.; Holt, H.; Kennedy, J. A. Interaction between grape-derived proanthocyanidins and cell wall material 2. Implications for vinification. *J. Agric. Food Chem.* **2010**, *58*, 10736–10746.
- (4) Le Bourvellec, C.; Le Quere, J.-M.; Renard, C. M. G. C. Impact of noncovalent interactions between apple condensed tannins and cell walls on their transfer from fruit to juice: studies in model suspensions and application. *J. Agric. Food Chem.* **2007**, *55*, 7896–904.



- (5) Renard, C. M. G. C.; Baron, A.; Guyot, S.; Drilleau, J. F. Interactions between apple cell walls and native apple polyphenols: quantification and some consequences. *Int. J. Biol. Macromol.* **2001**, *29*, 115–125.
- (6) Le Bourvellec, C.; Guyot, S.; Renard, C. M. G. C. Non-covalent interaction between procyanidins and cell wall material. Part I: Effect of some physicochemical parameters. *Biochim. Biophys. Acta* **2004**, *1672*, 192–202.
- (7) Kennedy, J. A.; Taylor, A. W. Analysis of proanthocyanidins by high-performance gel permeation chromatography. *J. Chromatogr., A* **2003**, *995*, 99–107.
- (8) Bindon, K. A.; Smith, P. A.; Kennedy, J. A. Interaction between grape-derived proanthocyanidins and cell wall material. I. Effect on proanthocyanidin composition and molecular mass. *J. Agric. Food Chem.* **2010**, *58*, 2520–2528.
- (9) Bindon, K. A.; Kennedy, J. A. Ripening-induced changes in grape skin proanthocyanidins modifies their interaction with cell walls. *J. Agric. Food Chem.* **2011**, *59*, 2696–2707.
- (10) Le Bourvellec, C.; Renard, C. M. G. C. Non-covalent interaction between procyanidins and cell wall material. Part II: Role of the cell wall structure. *Biochim. Biophys. Acta* **2005**, *1725*, 1–9.
- (11) Le Bourvellec, C.; Bouchet, B.; Renard, C. M. G. C. Non-covalent interaction between procyanidins and cell wall material. Part III: Study on model polysaccharides. *Biochim. Biophys. Acta* **2005**, *1725*, 10–18.
- (12) Nunan, K. J.; Sims, I. M.; Bacic, A.; Robinson, S. P.; Fincher, G. B. Changes in cell wall composition during ripening of grape berries. *Plant Physiol.* **1998**, *118*, 783–792.
- (13) Vicens, A.; Fournand, D.; Williams, P.; Sidhoum, L.; Moutounet, M.; Doco, T. Changes in polysaccharide and protein composition of cell walls in grape berry skin (cv. Shiraz) during ripening and over-ripening. *J. Agric. Food Chem.* **2009**, *57*, 2955–2960.
- (14) Ortega-Regules, A.; Ros-García, J. M.; Bautista-Ortin, A. B.; Lopez-Roca, J. M.; Gomez-Plaza, E. Changes in skin cell wall composition during the maturation of four premium wine grape varieties. *J. Sci. Food Agric.* **2008**, *88*, 420–428.
- (15) Hanlin, R. L.; Hrmova, M.; Harbertson, J. F.; Downey, M. O. Condensed tannin and grape cell wall interactions and their impact on tannin extractability into wine. *Aust. J. Grape Wine Res.* **2010**, *16*, 173–188.
- (16) Hazak, J. C.; Harbertson, J. F.; Lin, C. H.; Ro, B. H.; Adams, D. O. The phenolic components of grape berries in relation to wine composition. *Acta Hort.* (ISHS) **2005**, *689*, 189–196.
- (17) Vidal, S.; Williams, P.; O'Neill, M. A.; Pellerin, P. Polysaccharides from grape berry cell walls. Part I: Tissue distribution and structural characterization of the pectic polysaccharides. *Carbohydr. Polym.* **2001**, *45*, 315–323.
- (18) Kennedy, J. A.; Jones, G. P. Analysis of proanthocyanidin cleavage products following acid-catalysis in the presence of excess phloroglucinol. *J. Agric. Food Chem.* **2001**, *49*, 1740–1746.
- (19) González-Centeno, M. R.; Rosselló, C.; Simal, S.; Garau, M. C.; López, F.; Femenia, A. Physico-chemical properties of cell wall materials obtained from ten grape varieties and their byproducts: grape pomaces and stems. *LWT—Food Sci. Technol.* **2010**, *43*, 1580–1586.
- (20) Honda, S.; Akao, E.; Suzuki, E.; Okuda, M.; Kakehi, K.; Nakamura, J. High-performance liquid chromatography of reducing carbohydrates as strongly ultraviolet-absorbing and electrochemically sensitive 1-phenyl-3-methyl-5-pyrazolone derivatives. *Anal. Biochem.* **1989**, *180*, 351–357.
- (21) Filisetti-Cozzi, T. M. C. C.; Carpita, N. C. Measurement of uronic acids without interference from neutral sugars. *Anal. Biochem.* **1991**, *197*, 157–162.
- (22) Albersheim, P.; Nevins, D. J.; English, P. D.; Karr, A. A method for the analysis of sugars in plant cell-wall polysaccharides by gas-liquid chromatography. *Carbohydr. Res.* **1967**, *5*, 340–345.
- (23) Ciucanu, I.; Kerek, F. A simple and rapid method for the permethylation of carbohydrates. *Carbohydr. Res.* **1984**, *131*, 209–217.
- (24) Sims, I. A.; Bacic, A. Extracellular polysaccharides from suspension cultures of *Nicotiana plumbaginifolia*. *Phytochemistry* **1995**, *38*, 1397–1405.
- (25) Lau, E.; Bacic, A. Capillary gas chromatography of partially methylated alditol acetates on a high-polarity, cross-linked, fused-silica BPX70 column. *J. Chromatogr., A* **1993**, *637*, 100–103.
- (26) Goering, H. K.; van Soest, P. J. *Forage Fiber Analyses: Apparatus, Reagents, and Some Applications*; Agricultural Handbook 379; U.S. Department of Agriculture: Washington, DC, 1970; pp 1–20.
- (27) Van Soest, P. J.; Robertson, J. B.; Lewis, B. A. Methods for dietary fibre, neutral detergent fibre, and nonstarch polysaccharides in relation to animal nutrition. *J. Dairy Sci.* **1991**, *74*, 3583–3596.
- (28) Marles, M. A. S.; Coulman, B. E.; Bett, K. E. Interference of condensed tannin in lignin analyses of dry bean and forage crops. *J. Agric. Food Chem.* **2008**, *56*, 9797–9802.
- (29) Bravo, L.; Saura-Calixto, F. Characterization of dietary fiber and the *in vitro* indigestible fraction of grape pomace. *Am. J. Enol. Vitic.* **1998**, *49*, 135–141.
- (30) Llobera, A.; Canellas, J. Dietary fibre content and antioxidant activity of Manto Negro red grape (*Vitis vinifera*): pomace and stem. *Food Chem.* **2007**, *101*, 659–666.
- (31) Porter, L. J.; Hrstich, L. N.; Chan, B. G. The conversion of procyanidins and prodelphinidins to cyanidin and delphinidin. *Phytochemistry* **1986**, *25*, 223–230.
- (32) Gagné, S.; Saucier, C.; Gény, L. Composition and cellular localization of tannins in Cabernet Sauvignon skins during growth. *J. Agric. Food Chem.* **2006**, *54*, 465–471.
- (33) Zhao, J.; Pang, Y.; Dixon, R. A. The mysteries of proanthocyanidin transport and polymerization. *Plant Physiol.* **2010**, *153*, 437–443.
- (34) Apolinar-Valiente, R.; Romero-Cascales, I.; López-Roca, J. M.; Gómez-Plaza, E.; Ros-García, J. M. Application and comparison of four selected procedures for the isolation of cell-wall material from the skin of grapes cv. Monastrell. *Anal. Chim. Acta* **2010**, *660*, 206–210.
- (35) Brummell, D. A. Cell wall disassembly in ripening fruit. *Funct. Plant Biol.* **2006**, *33*, 103–119.
- (36) Rogiers, S. Y.; Greer, D. H.; Hatfield, J. M.; Orchards, B. A.; Keller, M. Mineral sinks within ripening grape berries (*Vitis vinifera* L.). *Vitis* **2006**, *45*, 115–123.
- (37) Storey, R. Potassium localization in the grape berry pericarp by energy-dispersive X-ray microanalysis. *Am. J. Enol. Vitic.* **1987**, *38*, 301–309.
- (38) Malovíková, A.; Rinaudo, M.; Milas, M. Comparative interactions of magnesium and calcium counterions with polygalacturonic acid. *Biopolymers* **1994**, *34*, 1059–1064.
- (39) Wehr, J. B.; Menzies, N. W.; Blamey, F. P. C. Alkali hydroxide-induced gelation of pectin. *Food Hydrocolloids* **2004**, *18*, 375–378.